Total-Body ^{18}F-FDG PET/CT in Autoimmune Inflammatory Arthritis at Ultra-Low Dose: Initial Observations

Yasser Abdelhafez[1,2], Siba P. Raychaudhuri*[3,4], Dario Mazza[1], Soumajyoti Sarkar[3], Heather L. Hunt[1], Kristin McBride[1], Mike Nguyen[1], Denise T. Caudle[1], Benjamin A. Spencer[1,5], Negar Omidvari[1,5], Heejung Bang[6], Simon R. Cherry[1,5], Lorenzo Nardo[1], Ramsey D. Badawi[1,5], and Abhijit J. Chaudhari*[1]

[1]*Department of Radiology, University of California Davis, Davis, California;* [2]*Nuclear Medicine Unit, South Egypt Cancer Institute, Assiut University, Assiut, Egypt;* [3]*Department of Internal Medicine-Rheumatology, University of California Davis, Davis, California;* [4]*Northern California Veterans Affairs Medical Center, Mather, California;* [5]*Department of Biomedical Engineering, University of California Davis, Davis, California; and* [6]*Department of Public Health Sciences, University of California Davis, Davis, California*

Autoimmune inflammatory arthritides (AIA), such as psoriatic arthritis and rheumatoid arthritis, are chronic systemic conditions that affect multiple joints of the body. Recently, total-body (TB) PET/CT scanners exhibiting superior technical characteristics (total-body coverage, geometric sensitivity) that could benefit AIA evaluation, compared with conventional PET/CT systems, have become available. The objectives of this work were to assess the performance of an ultra-low-dose, ^{18}F-FDG TB PET/CT acquisition protocol for evaluating systemic joint involvement in AIA and to report the association of TB PET/CT measures with joint-by-joint rheumatologic examination and standardized rheumatologic outcome measures. **Methods:** Thirty participants (24 with AIA and 6 with osteoarthritis) were prospectively enrolled in this single-center, observational study. All participants underwent a TB PET/CT scan for 20 min starting at 40 min after intravenous injection of 78.1 ± 4.7 MBq of ^{18}F-FDG. Qualitative and quantitative evaluation of ^{18}F-FDG uptake and joint involvement were performed from the resulting images and compared with the rheumatologic assessments. **Results:** TB PET/CT enabled the visualization of ^{18}F-FDG uptake at joints of the entire body, including those of the hands and feet, in a single bed position, and in the same phase of radiotracer uptake. A range of pathologies consistent with AIA (and non-AIA in the osteoarthritis group) were visualized, and the feasibility of extracting PET measures from joints examined by rheumatologic assessments was demonstrated. Of 1,997 evaluable joints, there was concordance between TB PET qualitative assessments and joint-by-joint rheumatologic evaluation in the AIA and non-AIA cohorts for 69.9% and 91.1% joints, respectively, and an additional 20.1% and 8.8% joints, respectively, deemed negative on rheumatologic examination showed PET positivity. On the other hand, 10.0% and 0% joints in the AIA and non-AIA cohorts, respectively, were positive on rheumatologic evaluation but negative on TB PET. Quantitative measures from TB PET in the AIA cohort demonstrated a moderate-to-strong correlation (Spearman $\rho = 0.53$–0.70, $P < 0.05$) with the rheumatologic outcome measures. **Conclusion:** Systemic joint evaluation in AIA (and non-AIA) is feasible with a TB PET/CT system and an ultra-low-dose protocol. Our results provide the foundation for future larger studies to evaluate the possible improvements in AIA joint assessment via the TB PET/CT technology.

Key Words: total-body PET/CT; autoimmune arthritis; rheumatoid arthritis; psoriatic arthritis; osteoarthritis

Received Dec. 30, 2021; revision accepted Apr. 18, 2022.

For correspondence or reprints, contact Abhijit J. Chaudhari (ajchaudhari@ucdavis.edu).

*Contributed equally to this work.

Published online May 19, 2022.

J Nucl Med 2022; 63:1579–1585
DOI: 10.2967/jnumed.121.263774

Autoimmune inflammatory arthritides (AIA), such as psoriatic arthritis (PsA) and rheumatoid arthritis (RA), are chronic, systemic conditions with articular and extraarticular manifestation. Joint inflammation is regarded as the hallmark of AIA and is considered a bellwether for downstream joint destruction and pain (*1*). Consequently, disease activity and treatment response assessments in AIA have relied primarily on the physical evaluation of joints (e.g., tenderness and swelling) and composite scores from joint examination, joint pain and activity, and laboratory inflammatory markers. These assessments, however, are subjective (*2*) and lack the sensitivity required to detect early or subclinical disease (*3*).

To address this limitation, PET/CT scanning using the radiotracer ^{18}F-FDG has been proposed, with results demonstrating the ability to assess joint inflammation (*4–8*), considered a precursor to AIA-associated joint damage. Despite these advantages, concerns about using ^{18}F-FDG PET/CT on current systems in the AIA population have been expressed. These include the significant cumulative dose to the patient for chronic disease activity monitoring or measuring treatment response (*9,10*) and the assessment of only portions of the body (e.g., just large joints (*11*)), given the limited PET sensitivity and spatial resolution characteristics of systems used for quantifying radiotracer uptake in small joints of the hands and feet that are affected early in AIA (*7,12*).

Recently, long-axial field-of-view (FOV) PET/CT systems capable of imaging either the entire adult human body (*13*) or large portions of the body (*14,15*) have become available. Their sensitivity characteristics are far superior to state-of-the-art conventional whole-body PET/CT systems, and early studies have shown that dose reduction is possible (*16*). These systems have a spatial resolution comparable to or better than conventional whole-body PET/CT scanners (*13*). To date, however, these total-body (TB) PET/CT systems have not been evaluated for assessing systemic autoimmune diseases, such as AIA.

In this article we present the first-in-humans evaluation of a TB PET/CT scanner to document the head-to-toe articular manifestations of AIA. The objectives of this work were to assess the performance of an ultra-low-dose ^{18}F-FDG TB PET/CT acquisition protocol to evaluate joint involvement in AIA and to report the association of rheumatologic measures of AIA joint and disease activity with those evaluated from TB PET/CT.

TABLE 1
Characteristics of the Study Participants and Summary of Their Rheumatologic Assessments

Characteristic	Non-AIA ($n = 6$)	AIA ($n = 24$)	P	AIA		P
				PsA ($n = 15$)	RA ($n = 9$)	
Age (y)	54.5 ± 14.5 (36–72)	58.5 ± 13.9 (28–77)	0.63	56.8 ± 16.3 (28–77)	61.4 ± 8.3 (47–71)	0.79
BMI (kg/m^2)	28.6 ± 8.4 (19.8–40)	31.3 ± 6.3 (20–46.6)	0.49	32.3 ± 7.1 (20–46.6)	29.6 ± 4.5 (23.1–36.4)	0.36
TJC (68 joints)	0.5 ± 0.8 (0–2)	12.5 ± 14 (0–55)	<0.001	10.5 ± 13.7 (0–55)	16 ± 14.4 (4–45)	0.22
SJC (68 joints)	0	1.6 ± 2.4 (0–9)	—	1.9 ± 2.7 (0–9)	1.2 ± 2.0 (0–6)	0.67
TJC (28 joints)	0	8.7 ± 7.1 (0–25)	—	7 ± 6.8 (0–25)	11.6 ± 7.1 (4–23)	0.13
SJC (28 joints)	0	1.2 ± 1.7 (0–6)	—	1.1 ± 1.6 (0–5)	1.2 ± 2.0 (0–6)	0.92
DAS-28-CRP*	—	3.7 ± 1.1 (2.1–5.4)	—	3.7 ± 1.1 (2.1–5.4)	3.7 ± 1.0 (2.4–5.1)	0.93

*DAS-28-CRP is not a validated outcome measure for non-AIA (OA) so was not calculated.
Values are reported as mean ± SD (minimum–maximum).
BMI = body mass index; TJC = tender joint count; SJC = swollen joint count; CRP = C-reactive protein.

MATERIALS AND METHODS

Study Participants

This prospective study was approved by Institutional Review Board of the University of California Davis, and all participants provided written informed consent before study procedures began. The recruited participants had a confirmed diagnosis, according to established criteria, of 1 of 2 subtypes of AIA (PsA or RA) (*17,18*) or osteoarthritis (OA), a non-AIA (*19*).

All study participants underwent rheumatologic evaluation by a fellowship-trained, board-certified rheumatologist and dermatologist with over 25 y of posttraining experience in AIA within 2 wk before the TB PET/CT scan. Rheumatologic assessments included the evaluation of 68 joints using the Disease Activity in Psoriatic Arthritis (DAPSA) outcome measure (*20*) and Disease Activity Score (based on the assessment of 28 joints [DAS-28] (*21*), which are subset of the 68 joints). Blood samples were drawn on the day of the scan for assessing serum C-reactive protein (CRP), used to calculate DAPSA score and DAS-28-CRP. The swollen and tender joint counts (swollen joint count, tender joint count) were recorded. A joint was considered positive if it was tender, swollen, or both.

Total-Body ^{18}F-FDG PET/CT

All participants underwent scanning on a TB PET/CT scanner (uEXPLORER; United Imaging Health Care) at a single time point for 20 min starting at 40 ± 1 min after an intravenous injection of 78.1 ± 4.7 MBq of ^{18}F-FDG. Details of

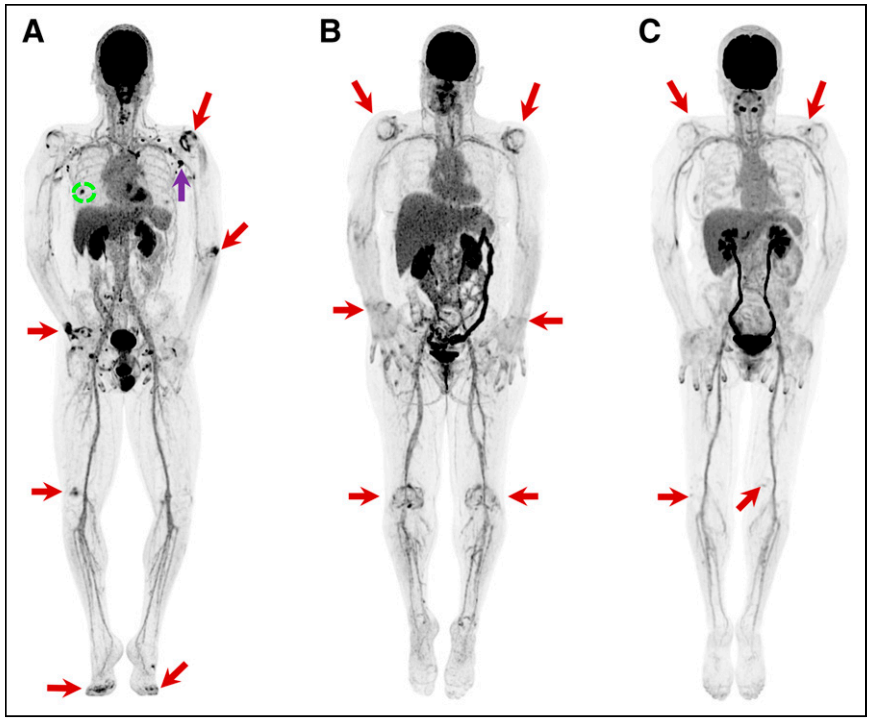

FIGURE 1. Total-body ^{18}F-FDG PET uptake in participants with AIA compared with those with OA, shown as maximum-intensity projections (MIPs). (A) A 33-y-old man with PsA, showing asymmetric polyarthritis involving left shoulder, left elbow, right wrist, right knee, and small joints of the hands and feet (arrows). (B) A 59-y-old woman with RA, showing mostly bilateral symmetric joint involvement of the shoulders and knees, and to lesser extent the wrist joints. (C) A 64-y-old woman with OA, presenting primarily mild-to-moderate uptake at fewer joints (shoulders and knees) commonly involved in this condition. Several extraarticular findings are noted in A, including ^{18}F-FDG–avid bilateral axillary and left supraclavicular lymph nodes. Left side uptake is secondary to COVID vaccination (purple arrow), and the active spot (dashed circle) seen opposite the inferior angle of the scapula corresponds to inflamed scapulothoracic bursa.

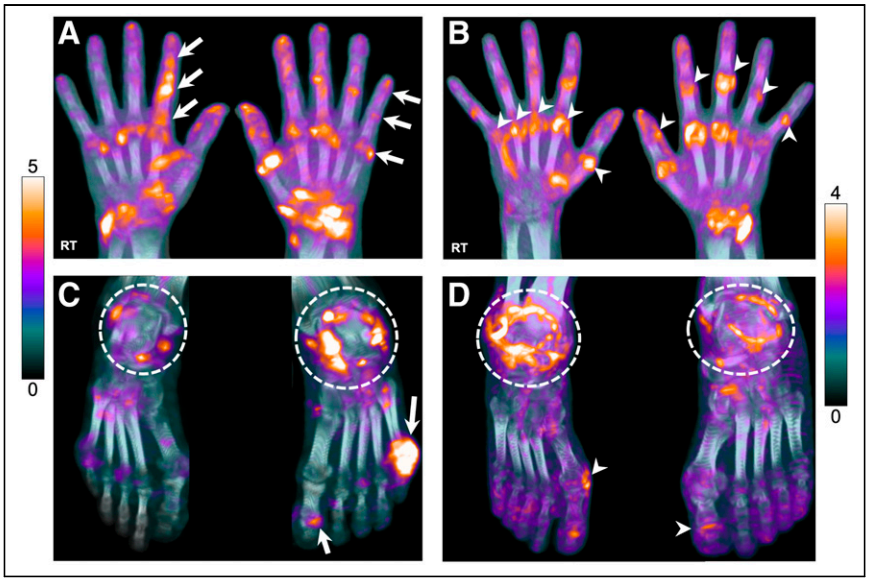

FIGURE 2. ^{18}F-FDG uptake in hands and feet of participants with AIA. (A) A 54-y-old man with PsA showing elevated uptake at multiple hand joints. Raylike distribution, as indicated by arrows, in metacarpophalangeal (MCP), proximal interphalangeal (PIP), and distal interphalangeal (DIP) joints in sequence, attributed to involvement of flexor or extensor tendons. (B) A 47-y-old woman with RA, showing involvement of entire row of MCP (arrowheads, right hand) and PIP/interphalangeal (IP) joints (arrowheads, left hand). (C) Feet images of same PsA participant in A, demonstrating increased uptake at ankle joints (dashed circles), more intense on the left side, and left first IP and fifth metatarsophalangeal (MTP) joints (arrows). (D) Feet images of a 71-y-old man with RA, demonstrating bilateral, rather symmetric, uptake around ankles as well as right first MTP and left first IP joints, suggestive of synovitis (arrowheads).

participant positioning, acquisition, reconstruction, and image assessment are provided in the supplemental materials (supplemental materials are available at http://jnm.snmjournals.org). TB PET/CT image assessments were reported qualitatively for each of the 68 joints using a modified 4-point Likert scale (*5*): 0, no uptake; 1, mild uptake comparable to the surrounding background; 2, moderate uptake higher than the surrounding background and comparable to blood pool (BP) at the ascending aorta; and 3, marked uptake higher than BP. For binary analyses, any uptake with a score of ≥ 2 was considered positive. SUV_{max} was measured on 2.344-mm isotropic voxel reconstructions with no point-spread function modeling or postprocessing smoothing. Measurements were performed only for joints that scored ≥ 1. Values were reported as a ratio ($rSUV_{max}$) between the joint SUV_{max} normalized by the BP SUV_{mean}. Positive joint count, summed qualitative scores, and summed $rSUV_{max}$ were derived for each scan. Further, a composite measure (PET_{comp}) was calculated analogous to the DAPSA score (*20*) as the sum of positive joints from PET, patient-reported outcomes of joint pain and activity (each between 1 to 10), and serum CRP level in mg/dL.

Statistical Analysis

Continuous variables were compared between 2 independent categoric groups using the Mann–Whitney *U* test. Association between categoric variables was assessed using the Fisher exact test. Correlation between 2 continuous measures was calculated using Spearman ρ. All analyses were performed using SPSS, version 21 (IBM Corp.).

RESULTS

Participant Characteristics

Thirty participants (24 with established AIA [15 PsA and 9 RA], and 6 with non-AIA [OA]; 7 women and 23 men), with a median age of 63.5 y (age range: 28–77 y), were evaluated. Characteristics of the participants and outcomes of their rheumatologic assessments are presented in Table 1. As expected, participants with AIA had higher positive joint counts than those without AIA. There was no difference in participant characteristics or rheumatologic assessments between individuals with PsA and RA.

TB PET/CT Systemic Joint Evaluation

All participants completed their TB PET/CT scans. Figure 1 shows PET maximum-intensity-projection (MIP) images for representative participants. Of a total of 2,040 joints (30 participants × 68 joints per participant), 43 (~2%) joints from 6 participants with AIA could not be adequately evaluated from the scans (due to prosthesis [8 joints], significant motion [30 joints], or being outside the PET and CT FOV [5 elbow joints]). Thus, the analysis presented is for 1,997 evaluable joints.

Most participants with AIA (23/24, 95.8%) presented with peripheral polyarthritis apparent on TB PET/CT. Figure 2 shows images of the hands and feet of representative study participants with AIA. Table 2 provides details of joints with positive TB PET/CT findings.

Comparison of TB PET/CT Assessments with Rheumatologic Outcome Measures

Qualitative Evaluation. In the AIA cohort, of 1,589 joints evaluated, 69.9% showed concordance between the TB PET and joint-by-joint rheumatologic evaluation (Table 3). An additional 20.1% were positive on TB PET but negative on rheumatologic examination. Finally, 10.0% were negative on TB PET but positive on rheumatologic evaluation. Supplemental Table 1 summarizes the distribution of the 159 joints in the latter category. Of these joints, 148 (93.0%) were small joints of the hands or feet, and 136 of the 148 joints (91.9%) were just tender on physical examination with no objective evidence of swelling or redness. In OA participants, concordance between TB PET and joint-by-joint rheumatologic evaluation was 91.2%. An additional 8.8% of joints were positive on TB PET but negative on rheumatologic examination, whereas no joints were negative on TB PET and positive on rheumatologic examination (Table 3).

Quantitative Evaluation. Quantitative ^{18}F-FDG TB PET/CT findings in joints are summarized in Table 4. Imaging metrics were higher in AIA participants than in non-AIA participants. Systemic ^{18}F-FDG TB PET metrics showed moderate-to-strong correlation with the DAPSA and DAS-28 scores (Table 5). The correlation coefficient was higher with DAS-28 because the measure does not involve assessment of the hand DIP or any foot joints.

DISCUSSION

We report articular findings from first-in-humans ^{18}F-FDG TB PET/CT scans in an AIA and non-AIA (OA) population. The entire adult human body was imaged in a single bed position in the same phase of radiotracer uptake. An ultra-low-dose protocol was implemented. The ability of assessing ^{18}F-FDG uptake for both large and small joints across the body was demonstrated.

Early diagnosis of AIA and initiation of treatment at its onset is essential to achieve clinical remission or at least low or minimal

TABLE 2
Frequency and Distribution of Positive Joints on ^{18}F-FDG TB PET/CT

Joint group	Specific joint(s)	Positive joint count/no. of participants (average)	
		Non-AIA	AIA
Hand joints	First IP and 2-fifth PIP	6/2 (3.0)	82/17 (4.8)
	1st-5th MCP	1/1 (1.0)	71/15 (4.7)
	2nd-5th DIP	0/0 (0)	38/10 (3.8)
	Sum	7/2 (3.5)	191/20 (9.6)
Feet joints	First IP, 2nd-5th PIP and DIP	0/0 (0)	15/5 (3.0)
	1st-5th MTP	4/3 (1.3)	41/10 (4.1)
	Sum	4/3 (1.3)	56/11 (5.1)
Upper limb joints	Gleno-humeral	6/4 (1.5)	37/21 (1.8)
	Acromio-clavicular	3/2 (1.5)	23/13 (1.8)
	Sterno-clavicular	3/3 (1.0)	26/17 (1.5)
	Elbows	3/2 (1.5)	11/8 (1.4)
	Wrists	4/2 (2.0)	31/19 (1.6)
	Sum	19/5 (3.8)	128/22 (5.8)
Lower limb joints	Hips	5/3 (1.7)	22/13 (1.7)
	Knees	1/1 (1.0)	20/14 (1.4)
	Talo-tibial	3/2 (1.5)	20/12 (1.7)
	Midtarsal and subtalar	0/0 (0)	17/12 (1.4)
	Sum	9/4 (2.3)	79/21 (3.8)
Temporomandibular joints		0/0 (0)	9/6 (1.5)
Sum of all positive joints/participants (average)		39/6 (6.5)	463/23 (20.1)

Data in parentheses are percentages.
IP = interphalangeal; PIP = proximal interphalangeal; MCP = metacarpophalangeal; DIP = distal interphalangeal; MTP = metatarsophalangeal.

disease activity (*22,23*). There is currently no validated diagnostic test for PsA (*24*), and clinical assessments for AIA are suboptimal (*2*). Therefore, the ability to perform a systemic evaluation of AIA-associated joint inflammatory activity in a quantitative manner on a per-patient basis via TB PET/CT, as demonstrated by our study, could offer an important tool to the rheumatology community. Furthermore, TB PET/CT could be useful to monitor response to therapies on a personalized basis and justify cessation, reduction or switching to another line of treatment (*24–26*). Beyond joints, TB PET/CT provides the visualization of other tissues that AIA may impact, such as the axial skeleton, entheses, digits (dactylitis), and nail and skin, as well as organs such as heart, brain, liver, kidneys, and skeletal muscle (*27,28*). Future investigations in assessing the impact of AIA on these tissues could further expand our understanding of the disease process.

Our findings indicate that 20.1% of AIA joints deemed negative on rheumatologic examination were PET-positive. This mismatch has also been reported by other PET studies (*4,8,29*). It is plausible

TABLE 3
Qualitative ^{18}F-FDG TB PET/CT Findings in Joints in Comparison with Rheumatologic Examination

^{18}F-FDG TB PET evaluation	Rheumatologic examination			
	AIA		Non-AIA	
	Negative	Positive (T/S/TS)	Negative	Positive (T/S/TS)
Negative	967	159 (146/4/9)	369	0
Positive	320	143 (117/3/23)	36	3 (3/0/0)
Total (n = 1997)*	1287	302	405	3

*Forty-three joints in AIA participants were unevaluable on PET; 6 of them were tender on rheumatologic examination.
T = only tender; S = only swollen; TS = tender and swollen.

TABLE 4
Quantitative Findings from ^{18}F-FDG TB PET/CT–Positive Joints

^{18}F-FDG PET metrics derived from …	Non-AIA (n = 6)	AIA (n = 24)	P
68 Joints			
Positive count	6.5 ± 4.9 (2–14)	19.3 ± 12.6 (0–49)	0.01
Summed scores	14.2 ± 10.7 (4–30)	44.5 ± 30.2 (0–124)	0.01
Summed $rSUV_{max}$	10.7 ± 8.7 (2.9–25.2)	28.6 ± 19.3 (1.5–90.2)	0.001
28 Joints			
Positive count	3.5 ± 2.7 (0–7)	10.7 ± 7.6 (0–26)	0.02
Summed scores	7.7 ± 5.9 (0–14)	24.1 ± 17.1 (0–64)	0.02
Summed $rSUV_{max}$	6.7 ± 4.1 (1.8–12.5)	16.3 ± 11.1 (4.2–50.3)	0.001

Values are reported as mean ± SD (minimum–maximum).
$rSUV_{max}$ = ratio between joint SUV_{max} and blood pool SUV_{mean}.

to hypothesize that ^{18}F-FDG PET, due to its ability to detect cellular metabolic activity, is sensitive to subclinical AIA inflammation that may be occult on rheumatologic evaluation but may play a role in joint damage (*30*). Future studies with short- and long-term follow-up will be needed to test this hypothesis. On the other hand, 10.0% joints that were positive on rheumatologic evaluation were PET-negative. There could be 3 possible reasons for this discrepancy. First, 93.6% of these joints were assessed as being tender on rheumatologic evaluation. Tenderness alone in established AIA may not reflect active inflammation (*31–33*). Furthermore, inclusion of the tender joint count in rheumatologic assessment may confound evaluation of AIA inflammatory activity (*34*). Our results support this premise and could help better establish the clinical value of tenderness in AIA evaluation, with or without synovitis or swelling. The second reason could be the limited TB PET spatial resolution (~3 mm (*13*)) for the small joints of the hand and feet. The reconstructed radiotracer uptake was likely underestimated for the small joints; data suggest that the contrast recovery coefficient for a 10-mm sphere with 4-to-1 source-to-background ratio and using the same reconstruction method used here is approximately 50% (*13*). The quantification of small lesion activity could likely be improved with the implementation of advanced image reconstruction methods developed specifically for TB PET/CT (*35*). Spatial resolution is particularly important in AIA imaging, as AIA may coexist with OA or another musculoskeletal condition in the same anatomic region (e.g., small joints of the hand (*7*)), and defining the pattern may be critical for differential diagnosis (*22*). Finally, despite the use of positioning aids, intrascan motion likely confounded the evaluation of the small joints of the hand and feet. Impact of motion could be mitigated by shortening image acquisition time or retrospective temporal binning of the data into shorter frames and either software-driven motion correction or choosing frames with the least intrascan motion (*36*). For shortening the image acquisition time while maintaining the signal-to-noise ratio, an increase in the injected dose may be necessary. On the other hand, advanced low-count image reconstruction methods (*35*) will be essential when using short frames.

TABLE 5
Spearman Correlation (ρ) Between Systemic Joint Measures from ^{18}F-FDG TB PET/CT and Rheumatologic Assessments

	Rheumatologic assessments	
^{18}F-FDG PET metrics	DAPSA score (n = 15 with PsA)	DAS-28-CRP (n = 24 with AIA)
68 Joints		
Positive count	0.61* (0.10–0.88)	0.62† (0.30–0.82)
Summed scores	0.61* (0.08–0.89)	0.61† (0.27–0.83)
Summed $rSUV_{max}$	0.56* (0.03–0.86)	0.53† (0.18–0.77)
PET_{comp}‡	0.63* (0.17–0.87)	0.70* (0.40–0.86)
28 Joints		
Positive count	0.55* (0.06–0.89)	0.68† (0.40–0.86)
Summed scores	0.57* (0.09–0.89)	0.68† (0.39–0.87)
Summed $rSUV_{max}$	0.53* (0.01–0.87)	0.60† (0.29–0.84)

*$P < 0.05$.
†$P < 0.01$.
‡PET_{comp} = positive joint count + patient-reported joint activity + patient-reported joint pain + CRP.
Values are given as Spearman ρ-coefficient (with 95% CIs in parentheses). Because DAPSA score is not validated for evaluating RA, data under the DAPSA column are extracted from participants with PsA, whereas data under DAS-28-CRP are extracted from all the 24 participants with AIA.

Because of the high sensitivity of the TB PET/CT system (*13*), an ultra-low-dose protocol was implemented. Our findings are overall consistent with documented patterns of joint involvement in AIA, and with the findings of previous studies (*4–6,8,37,38*), though those studies used a 3- to 5-times higher injected dose than that used in our study. Dose is a significant limitation for the broader adoption of PET/CT technology in AIA (*9,10*), given its chronic nature and the potential need for monitoring disease activity in both treatment responders and nonresponders. Low-dose approaches such as those used in our work could therefore provide means for the rheumatology community to capitalize on the benefits offered by TB PET/CT.

A 40-min ^{18}F-FDG uptake time was used based on the tracer's arterial blood clearance characteristics (*39,40*), with a 20-min scan time, and data were reconstructed into a single frame matching our current clinical protocols (*41*). Our pilot data recently showed that shorter scans may provide reasonable image quality (*42*). These shorter scans need further validation; however, they could motivate

the creation of more practical scanning protocols suitable for the AIA population that experiences significant difficulty in tolerating long scan times. The shorter frames could also enable future classification of ^{18}F-FDG kinetics in lesions over the 20-min window and provide additional biomarkers, such as those from relative Patlak plots (*43*). Furthermore, the 40- to 60-min scanning window used will allow future exploration of optimizing the scan start time within that window.

Our study has limitations. First, this was a feasibility study with a modest sample size. Second, this was a cross-sectional study with participants enrolled with different levels of AIA disease activity, and the treatments they were receiving could have affected the PET findings. Follow-up TB PET imaging will be essential to establish the test–retest reliability in this patient population. Third, semiquantitative SUV_{max}-based measures were used and other measures, such as metabolically active volume, can be considered in the future. Fourth, our ultra-low-dose CT protocol, while supporting PET attenuation correction and anatomic localization, resulted in an overall low CT image quality. An increase in dose and deployment of recently developed machine-learning–based methods for low-dose CT reconstruction (*44*) could be helpful to address this limitation and to assess the added value of CT-based joint findings. Fifth, the transaxial FOV was not sufficient to capture the elbows consistently. Positioning schemes that would enable the capture of all joints of the body will be helpful to implement in the future. Sixth, the study was not powered to assess differences in PET uptake patterns between the AIA subtypes. Finally, we did not compare our findings with those from other imaging modalities such as ultrasound or MRI. These studies could help define the future role of TB PET/CT for AIA assessment compared with other imaging modalities.

CONCLUSION

The feasibility of acquiring ^{18}F-FDG TB PET/CT scans in participants with AIA, and a non-AIA comparator group, at an ultra-low dose was demonstrated. TB PET/CT enabled the acquisition of joints of the entire body, including hands and feet, in a single bed position, and in the same phase of radiotracer uptake. A range of pathologies consistent with AIA (and non-AIA) were visualized, and the feasibility of extracting PET measures from anatomic sites commonly examined clinically (68 and 28 joints) was demonstrated. Quantitative measures from TB PET/CT demonstrated a moderate-to-strong correlation with outcomes of AIA rheumatologic assessments. These results provide the foundation for future studies to substantiate these findings and quantitatively evaluate the improvements possible in AIA assessment via the TB PET/CT technology.

DISCLOSURE

University of California Davis has a research and a revenue-sharing agreement with United Imaging Health Care. Ramsey D. Badawi, Simon R. Cherry, and Lorenzo Nardo are investigators on a research grant funded by United Imaging Health Care, the manufacturer of the scanner used in this article. The work is supported in part by the National Institutes of Health (NIH R01 AR076088 and R01 CA206187) and the National Psoriasis Foundation. No other potential conflict of interest relevant to this article was reported.

ACKNOWLEDGMENTS

We thank Dr. Fatma Sen, Mr. John Brock, Mr. Ofilio Vigil, Ms. Lynda Painting, and Ms. Dana Little from the University of California, Davis for their support.

KEY POINTS

QUESTION: Is it feasible to assess joint involvement in autoimmune arthritis using ^{18}F-FDG and an ultra-low-dose protocol on a TB PET/CT scanner?

PERTINENT FINDINGS: In this prospective study, systemic joint involvement in participants with autoimmune arthritis was successfully visualized and ^{18}F-FDG uptake per joint was quantified. Results showed a high concordance of TB PET/CT measures with joint-by-joint rheumatologic evaluation and moderate-to-strong correlation with rheumatologic outcome measures. ^{18}F-FDG TB PET/CT was positive for 20% of joints deemed negative on rheumatologic examination, suggestive of its ability to potentially detect subclinical disease activity.

IMPLICATIONS FOR PATIENT CARE: Evaluation of autoimmune arthritis is feasible using ultra-low-dose, ^{18}F-FDG TB PET/CT scans.

REFERENCES

1. Sweeney SE, Firestein GS. Rheumatoid arthritis: regulation of synovial inflammation. *Int J Biochem Cell Biol.* 2004;36:372–378.
2. Pincus T. Limitations of a quantitative swollen and tender joint count to assess and monitor patients with rheumatoid arthritis. *Bull NYU Hosp Jt Dis.* 2008;66:216–223.
3. Hensor EMA, Conaghan PG. Time to modify the DAS28 to make it fit for purpose(s) in rheumatoid arthritis? *Expert Rev Clin Immunol.* 2020;16:1–4.
4. Beckers C, Ribbens C, Andre B, et al. Assessment of disease activity in rheumatoid arthritis with ^{18}F-FDG PET. *J Nucl Med.* 2004;45:956–964.
5. Goerres GW, Forster A, Uebelhart D, et al. F-18 FDG whole-body PET for the assessment of disease activity in patients with rheumatoid arthritis. *Clin Nucl Med.* 2006;31:386–390.
6. Yamashita H, Kubota K, Mimori A. Clinical value of whole-body PET/CT in patients with active rheumatic diseases. *Arthritis Res Ther.* 2014;16:423.
7. Chaudhari AJ, Ferrero A, Godinez F, et al. High-resolution ^{18}F-FDG PET/CT for assessing disease activity in rheumatoid and psoriatic arthritis: findings of a prospective pilot study. *Br J Radiol.* 2016;89:20160138.
8. Lee SJ, Jeong JH, Lee CH, et al. Development and validation of an ^{18}F-fluorodeoxyglucose-positron emission tomography with computed tomography-based tool for the evaluation of joint counts and disease activity in patients with rheumatoid arthritis. *Arthritis Rheumatol.* 2019;71:1232–1240.
9. McQueen FM. Imaging in early rheumatoid arthritis. *Best Pract Res Clin Rheumatol.* 2013;27:499–522.
10. Bruijnen ST, Gent YY, Voskuyl AE, Hoekstra OS, van der Laken CJ. Present role of positron emission tomography in the diagnosis and monitoring of peripheral inflammatory arthritis: a systematic review. *Arthritis Care Res (Hoboken).* 2014;66:120–130.
11. Kubota K, Ito K, Morooka M, et al. FDG PET for rheumatoid arthritis: basic considerations and whole-body PET/CT. *Ann N Y Acad Sci.* 2011;1228:29–38.
12. Narayan N, Owen DR, Taylor PC. Advances in positron emission tomography for the imaging of rheumatoid arthritis. *Rheumatology (Oxford).* 2017;56:1837–1846.
13. Spencer BA, Berg E, Schmall JP, et al. Performance evaluation of the uEXPLORER total-body PET/CT scanner based on NEMA NU 2-2018 with additional tests to characterize PET scanners with a long axial field of view. *J Nucl Med.* 2021;62:861–870.
14. Karp JS, Viswanath V, Geagan MJ, et al. PennPET Explorer: design and preliminary performance of a whole-body imager. *J Nucl Med.* 2020;61:136–143.
15. Prenosil GA, Sari H, Fürstner M, et al. Performance characteristics of the Biograph Vision Quadra PET/CT system with a long axial field of view using the NEMA NU 2-2018 standard. *J Nucl Med.* 2022;63:476–484.
16. Hu Y, Liu G, Yu H, et al. Feasibility of ultra-low ^{18}F-FDG activity acquisitions using total-body PET/CT. *J Nucl Med.* 2022;63:959–965.
17. Taylor W, Gladman D, Helliwell P, et al. Classification criteria for psoriatic arthritis: development of new criteria from a large international study. *Arthritis Rheum.* 2006;54:2665–2673.
18. Aletaha D, Neogi T, Silman AJ, et al. 2010 Rheumatoid arthritis classification criteria: an American College of Rheumatology/European League Against Rheumatism collaborative initiative. *Arthritis Rheum.* 2010;62:2569–2581.

19. Kolasinski SL, Neogi T, Hochberg MC, et al. 2019 American College of Rheumatology/Arthritis Foundation guideline for the management of osteoarthritis of the hand, hip, and knee. *Arthritis Care Res (Hoboken).* 2020;72:149–162.
20. Smolen JS, Breedveld FC, Burmester GR, et al. Treating rheumatoid arthritis to target: 2014 update of the recommendations of an international task force. *Ann Rheum Dis.* 2016;75:3–15.
21. Prevoo ML, van 't Hof MA, Kuper HH, van Leeuwen MA, van de Putte LB, van Riel PL. Modified disease activity scores that include twenty-eight-joint counts. Development and validation in a prospective longitudinal study of patients with rheumatoid arthritis. *Arthritis Rheum.* 1995;38:44–48.
22. Gossec L, Smolen JS, Ramiro S, et al. European League Against Rheumatism (EULAR) recommendations for the management of psoriatic arthritis with pharmacological therapies: 2015 update. *Ann Rheum Dis.* 2016;75:499–510.
23. Smolen JS, Landewe RBM, Bijlsma JWJ, et al. EULAR recommendations for the management of rheumatoid arthritis with synthetic and biological disease-modifying antirheumatic drugs: 2019 update. *Ann Rheum Dis.* 2020;79:685–699.
24. Ng BCK, Jadon DR. Unmet needs in psoriatic arthritis. *Best Pract Res Clin Rheumatol.* 2021;35:101693.
25. Bouman CA, van Herwaarden N, van den Hoogen FH, et al. Long-term outcomes after disease activity-guided dose reduction of TNF inhibition in rheumatoid arthritis: 3-year data of the DRESS study—a randomised controlled pragmatic non-inferiority strategy trial. *Ann Rheum Dis.* 2017;76:1716–1722.
26. Merola JF, Lockshin B, Mody EA. Switching biologics in the treatment of psoriatic arthritis. *Semin Arthritis Rheum.* 2017;47:29–37.
27. Figus FA, Piga M, Azzolin I, McConnell R, Iagnocco A. Rheumatoid arthritis: extra-articular manifestations and comorbidities. *Autoimmun Rev.* 2021;20:102776.
28. Van den Bosch F, Coates L. Clinical management of psoriatic arthritis. *Lancet.* 2018;391:2285–2294.
29. Kothekar E, Revheim ME, Borja AJ, et al. Utility of FDG-PET/CT in clinical psoriasis grading: the PET-PASI scoring system . *Am J Nucl Med Mol Imaging.* 2020;10:265–271.
30. Suto T, Okamura K, Yonemoto Y, Okura C, Tsushima Y, Takagishi K. Prediction of large joint destruction in patients with rheumatoid arthritis using ^{18}F-FDG PET/CT and disease activity score. *Medicine (Baltimore).* 2016;95:e2841.
31. Collison J. Tender joints might not indicate inflammation. *Nat Rev Rheumatol.* 2019;15:2.
32. Gessl I, Popescu M, Schimpl V, et al. Role of joint damage, malalignment and inflammation in articular tenderness in rheumatoid arthritis, psoriatic arthritis and osteoarthritis. *Ann Rheum Dis.* 2021;80:884–890.
33. Felbo SK, Wiell C, Østergaard M, et al. Do tender joints in active psoriatic arthritis reflect inflammation assessed by ultrasound and magnetic resonance imaging? *Rheumatology (Oxford).* 2022;61:723–733.
34. Hammer HB, Michelsen B, Provan SA, et al. Tender Joint count and inflammatory activity in patients with established rheumatoid arthritis: results from a longitudinal study. *Arthritis Care Res (Hoboken).* 2020;72:27–35.
35. Qi J, Matej S, Wang G, Zhang X. 3D/4D reconstruction and quantitative total body imaging. *PET Clin.* 2021;16:41–54.
36. Berg E, Revilla EM, Abdelhafez YG, et al. Framework design for comprehensive patient motion compensation in total-body PET [abstract]. Presented at: the virtual meeting of the IEEE Nuclear Science Symposium & Medical Imaging Conference, November 4–8, 2020. https://www.eventclass.org/contxt_ieee2020/online-program/session?s=M-10. Accessed September 2, 2022.
37. Roivainen A, Parkkola R, Yli-Kerttula T, et al. Use of positron emission tomography with methyl-^{11}C-choline and 2-^{18}F-fluoro-2-deoxy-D-glucose in comparison with magnetic resonance imaging for the assessment of inflammatory proliferation of synovium. *Arthritis Rheum.* 2003;48:3077–3084.
38. Kubota K, Ito K, Morooka M, et al. Whole-body FDG-PET/CT on rheumatoid arthritis of large joints. *Ann Nucl Med.* 2009;23:783–791.
39. Vriens D, de Geus-Oei LF, Oyen WJ, Visser EP. A curve-fitting approach to estimate the arterial plasma input function for the assessment of glucose metabolic rate and response to treatment. *J Nucl Med.* 2009;50:1933–1939.
40. Keramida G, Anagnostopoulos CD, Peters AM. The extent to which standardized uptake values reflect FDG phosphorylation in the liver and spleen as functions of time after injection of ^{18}F-fluorodeoxyglucose. *EJNMMI Res.* 2017;7:13.
41. Ng QK, Triumbari EKA, Omidvari N, Cherry SR, Badawi RD, Nardo L. Total-body PET/CT: first clinical experiences and future perspectives. *Semin Nucl Med.* 2022;52:330–339.
42. Abdelhafez Y, Hunt H, Caudle D, et al. Ultra-low-dose total-body ^{18}F-FDG PET/CT in patients with autoimmune inflammatory arthritis: evaluation of image quality with shorter scan time. *J Nucl Med.* 2021;62:1697.
43. Zuo Y, Qi J, Wang G. Relative Patlak plot for dynamic PET parametric imaging without the need for early-time input function. *Phys Med Biol.* 2018;63:165004.
44. Wu D, Kim K, El Fakhri G, Li Q. Iterative low-dose CT reconstruction with priors trained by artificial neural network. *IEEE Trans Med Imaging.* 2017;36:2479–2486.